Molecular Level Investigation of Organization in Ternary Lipid Bilayer: A Computational Approach

Sumita Mondal and Chaitali Mukhopadhyay*

Department of Chemistry, University of Calcutta, 92, A. P. C. Road, Kolkata 700 009, India

Received November 6, 2007. Revised Manuscript Received June 26, 2008

The differential organization of lipid components in a multicomponent membrane leads to formation of domains having diverse composition and size. Cholesterol and glycosphingolipids are known to be important components of such lateral assembly. We report here the ordering of cholesterol around ganglioside GM1 and the nature of the cluster from an all-atom simulation of a ternary lipid system. The results are compared with a binary bilayer and a pure phospholipid bilayer. The difference in molecular rearrangements in ternary and binary lipid mixture shows the role of GM1 in the rearrangement of cholesterol. Calculation of the radial distribution function, rotational reorientation, and residence time analysis of cholesterol shows that cholesterol is preferentially accumulating near gangliosides, while the lateral translational motion, rotational diffusion, and order parameter of phospholipids characterize the amount of rigidity imparted on the phospholipid bilayer.

Introduction

Current understanding of the cell surface membrane suggests that there can be immiscible gel and fluid lipid domains in the membrane arising out of the lateral arrangements of different membrane components. Phase separation in a multicomponent membrane is an important process required for formation of such lateral assemblies. Rafts, often described as lateral assemblies of lipids enriched in cholesterol (Chol) and sphingolipids, have been implicated to facilitate selective protein−protein interaction where different receptors and protein accumulate[1,2] and initiate signal transduction.[3,4] The existence and physical properties of such lipid are under rigorous study.[5,6] Experimental evidence indicates that these domains can vary not only in composition but also in size. Lipid domains of a large distribution in size, ranging from as large as 200 to ∼10−40 nm at the physiological temperature, are observed.[7] The existence of even small (∼5 nm) Chol-sensitive nanoclusters has been reported from a combination of computational study and fluorescence resonance energy transfer (FRET) measurements.[8] This heterogeneity of structure as well as composition of the membrane domains results from varying degrees of anomalous diffusion. Experimental evidence suggests that the physical state of such microdomains (liquid-ordered phase, L_o) are structurally and dynamically distinct from the rest of the membrane (liquid-disorderd phase, L_d).[9−13]

Chol and sphingolipids are another kind of lipids, known to be important components of lipid microdomains. It is well known that the presence and concentration of Chol are crucial factors for formation and size of the domains.[2,7] The long chain sphingolipids, i.e., ceramides, most abundant in nature and classified as "insoluble nonswelling amphiphiles", can aid to formation of highly ordered microdomains.[14−17] One of the major classes of sphingolipids are sialic acid-containing gangliosides abundant in neuron plasma membrane[18] and located at the outer-membrane surface asymmetrically with the hydrophilic sugar rings exposed in water and the hydrophobic ceramide part embedded in the lipid core. Gangliosides participate in a variety of cell surface events such as receptor and recognition phenomena, ion binding and release, and transduction of membrane-mediated information.[19] One of the most studied gangliosides is GM1 (ganglioside-monosialated) (Figure 1A), which can be incorporated up to 30 mol % in the membrane and acts as receptor for *Vibrio cholera* toxin and *Escheriachia coli* heat-labile enterotoxin.[20]

Though both the Chol and sphingolipids are known to be crucial components of membrane domains, little is known about the molecular level interactions between these two molecules in the lipid environment. We have recently shown evidence of stepwise formation of a Chol-rich domain in a bicomponent membrane bilayer.[21] We report here the effect of glycosphingolipids on other components of the membrane by the molecular dynamics simulation method. From the simulations the preference for Chol-GM1 pairing, changes in

* To whom correspondence should be addressed. Phone: 91-33-2350-8386. Fax: 91-33-2351-9755. E-mail: chaitalicu@yahoo.com, cmchem@caluniv.ac.in.

(1) Simons, K.; Vaz, V. L. *Annu. Rev: Biophys. Biomol. Struct.* **2004**, *33*, 269–295.
(2) Abankwa, D.; Gorfe, A. A.; Hancock, J. F. *Seminars Cell Dev. Biol.* **2007**, *18*, 599–607.
(3) Chiantia, S.; Kahya, N.; Schwille, P. *Langmuir* **2007**, *23*, 7659–7665.
(4) Kusumi, A.; Koyama-Honda, I.; Suzuki, K. *Traffic* **2004**, *5*, 213–230.
(5) Munro, S. *Cell* **2003**, *115*, 377–388.
(6) Nichols, B. *Nature* **2005**, *436*, 638–639.
(7) Hancock, J. F. *Nat. Rev. Mol. Cell Biol.* **2006**, *7*, 456–462.
(8) Sharma, P.; Varma, R.; Sarasij, R.; Ira, C.; Gousset, K.; Krishnamoorthy, G. *Cell* **2004**, *116*, 577–589.
(9) Johnston, L. J. *Langmuir* **2007**, *23*, 5886–5895.
(10) Jensen, M. H.; Morris, E. J.; Simonsen, A. C. *Langmuir* **2007**, *23*, 8135–8141.
(11) Coban, O.; Burger, M.; Laliberte, M.; Ianoul, A.; Johnston, L. J. *Langmuir* **2007**, *23*, 6704–6711.
(12) Veatch, S. L.; Leung, S. S. W.; Hancock, R. E. W.; Thewalt, L. *J. Phys. Chem. B* **2007**, *111*, 502–504.
(13) McQuaw, C. M.; Zheng, L.; Ewing, A. G.; Winograd, N. *Langmuir* **2007**, *23*, 5645–5650.
(14) Kolesnick, R. N.; Goni, F. M.; Alonso, A. *J. Cell Physiol.* **2000**, *184*, 285–300.
(15) Bollinger, C. R.; Teichgraber, V.; Gulbins, E. *Biochim. Biophys. Acta* **2005**, *1746*, 284–294.
(16) Chiantia, S.; Kahya, N.; Ries, J.; Schwille, P. *Biophys. J.* **2006**, *90*, 4500–4508.
(17) Holopainen, J. M.; Angelova, M. I.; Kinnunen, P. K. *Biophys. J.* **2000**, *78*, 830–838.
(18) Chatterjee, C.; Mukhopadhyay, C. *J. Biomol. Struct. Dyn.* **2005**, *23*, 183–192.
(19) Hirai, M.; Iwase, H.; Hayakawa, T.; Koizumi, M.; Takahashi, H. *Biophys. J.* **2003**, *85*, 1600–1610.
(20) Sonnino, S.; Mauri, L.; Chigorno, V.; Prinetti, A. *Glycobiology* **2007**, *17*, 1R–13R.
(21) Mondal, S.; Mukhopadhyay, C. *Chem. Phys. Lett.* **2007**, *439*, 166–170.

10.1021/la8015589 CCC: $40.75
Published on Web 08/20/2008

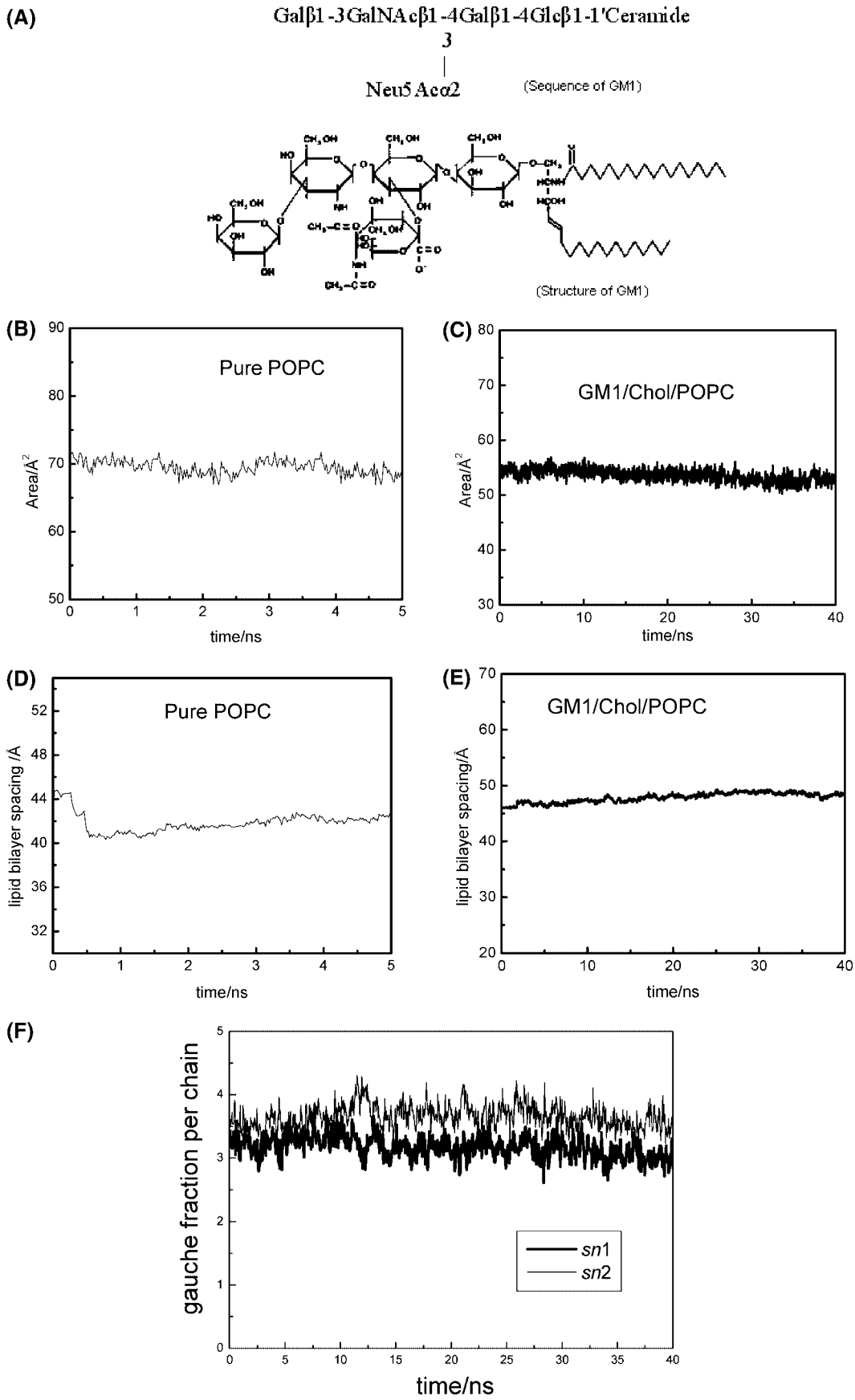

Figure 1. (A) Sequence (obtained from www.neuro.wustl.edu) and structure (obtained from www.cyberlipid.org/glycolip/glyl0036.htm) of GM1 (hydrogen atoms omitted). The time-dependent variation of (B, C) the surface area, (D, E) lateral spacing ($d-d$ spacing) for POPC in pure POPC and ternary lipid bilayer, and (F) number of gauche fractions per chain for POPC in GM1/Chol/POPC ternary lipid bilayer.

the dynamics of the membrane constituents, as well as several structural and dynamical parameters of the individual components are calculated to explain their combined effect on the PC bilayer. Results have been compared with pure PC bilayer

data as well as with bilayer containing Chol at two different concentrations.[21]

Modeling and Simulation Protocol

A pure lipid bilayer of 84 POPC molecules was constructed from the all-atom residue topology file of the CHARMM package[22] (version 31b1). The initial surface area of each PC monomer was 68 Å^2 (the reported value being 68.3 ± 1.5 Å^2 [23]). The method of bilayer construction was followed as reported by Wolf and Roux.[24,25] Briefly, a starting configuration for a phospholipid system was prepared from random selection of lipids from a pre-equilibrated, prehydrated set and then placing them in a bilayer. The short contacts between heavy atoms were reduced through systematic rotations (around the *z* axis) and translations (in the *xy* plane) of the lipids. A total of 3215 TIP3P water molecules in a orthorhombic water box of dimensions 60 Å × 60 Å × 84 Å were used to solvate the bilayer, and bad contacts were removed by deleting water within 2.6 Å from the lipid molecules. The solvated bilayer was equilibrated for 1 ns and simulated for 5 ns at 298 K (above the phase transition temperature for PC).[26] Twenty four Chol and 4 GM1 molecules were added to the POPC bilayer by systematically replacing POPC molecules. Chols were distributed in both the lower and upper layers, whereas GM1 was added only in the upper layer. As the area of Chol is approximately one-half the area of POPC, in each layer 12 Chol replaced 6 PC molecules. In the upper layer 4 GM1 replace 4 PC molecules with the pentasaccharide headgroup exposed to water and ceramide tail inserted into the bilayer. The area of the ceramide tail is close to the area of POPC tails.[27] To maintain neutrality 4 Na^+ ions were added. Coordinates of Chol atoms were obtained from Zoe et al.,[28] and the model of GM1 was constructed by patching the ceramide tail[29] with the GM1 head of 5 sugar rings obtained from the PDB structure of cholera toxin bound GM1 (pdb code 2chb.pdb) (Figure 1A). The system is next energy minimized by the ABNR (adopted basis Newton−Raphson) method and equilibrated for 5 ns. A 40 ns MD simulation run at NPT ensemble is performed using the Leap Verlet algorithm applying image in all three directions at 298 K. No constraints on surface tension were applied. In the initial step of the NPT run, a constrain was imposed on the PC lipid headgroup which was relaxed slowly within 1 ns run time. The Berendsen piston is used to keep the pressure constant at 1 atm. The grid spacing was kept below 0.34 Å, and a forth-order spline was used for the interpolation. The SHAKE algorithm was used to constrain all bonds in the system, allowing an integration time step of 2 fs. The long-range electrostatic interaction was handled with the particle mesh Ewald (PME) method with a real-space cutoff of 12 Å.[29,30] The van der Waals interactions were cutoff at 12 Å using a switching function from 10 Å. The last 30 ns data is taken for the analysis, leaving the initial 10 ns NPT run for establishing the equilibration.

Results and Discussion

The POPC molecule was used as the major constituent of the bilayer as this particular PC is abundant in the neuronal membranes.[31] The NPT ensemble and CHARMM force field have been shown earlier to successfully model the lipid bilayers.[27,32,33] To check the stability and quality of the simulation, several quantities were monitored. The total energy conservation is fairly good with fluctuations less than 10^{-4} kcal/mol. No temperature drift was observed during the entire run. The time course of the average surface area per PC (Figure 1B and 1C) and *d*−*d* spacing (Figure 1D and 1E) for pure POPC and mixed lipid bilayers clearly indicate the well equilibration of both the systems. The surface area is calculated following the method of Hofsab et al.[34] The volume of water is subtracted from the total volume of the system to get the volume of lipid which was divided by bilayer spacing and number of lipids to get the area per POPC for pure PC bilayer. To get the volume of PC for mixed lipid bilayer, the volume of GM1 and Chol were calculated and subtracted from the total volume of lipid. The volume of GM1 is calculated from the procedure of Wolf and Roux,[24,25] and the volume of Chol is obtained from literature data.[34] The average surface area computed for pure POPC bilayer is 70 ± 2 Å^2, which is in very good agreement with the experimental value[23] of 68.3 ± 1.5 Å^2. The average surface area for the mixed bilayer containing GM1 and Chol is 53 ± 2 Å^2. For the binary bilayer containing only POPC and cholesterol (33 mol %) the average surface area was obtained to be 54 ± 2 Å^2 (data not shown). It was reported earlier that for 40 mol % Chol concentration in binary lipid bilayer conaining Chol and POPC the area is approximately 57 Å^2.[35] The average *d*−*d* spacing is calculated by measuring the time averages of the P−P distance from both the leaflets to be 41 ± 1 Å, close to the literature data of 39 Å,[36] and practically remains constant after 1 ns. In the ternary bilayer the value changes to 48 ± 1 Å, which is expected as the surface area is getting reduced. The number of gauche fractions per chain (Figure 1F) for mixed bilayer is calculated by counting the total number of gauche conformations per chain with time.[36] This gives approximately the value of 3.2 ± 0.2 for *sn1* chain and 3.8 ± 0.2 for *sn2* chain with moderate fluctuation throughout the simulation. The literature data available for pure POPC bilayer is 3.0 and 3.2 for *sn1* and *sn2* chains, respectively.[36] A decrease in surface area and an increase in *d*−*d* spacing and gauche fraction per chain for both *sn1* and *sn2* chain are indicative of an increase of rigidity in the presence of Chol and GM1.

We wanted to verify if there is any specific interaction between GM1 and Chol which might lead to cluster formation. How does the presence of GM1 in the upper leaflet affect the structure and dynamics of Chol and POPC in both layers? Is GM1-Chol pairing preferred over Chol-POPC pairing? Finally, how do the properties of the ternary layers compare with that of pure POPC and POPC-Chol binary layers?

The presence of GM1 in the upper layer makes the membrane bilayer asymmetric. However, this does not destabilize the system as the bulky pentasaccharide headgroup of GM1 faces the water layer. This causes the water distribution to become asymmetric. In Figure 2 we see the distribution of various constituents of the

(22) MacKerell, A. D., Jr.; Bashford, D.; Bellott, M.; Dunbrack, R. L., Jr.; Evanseck, J. D.; Field, M. J.; Fischer, S.; Gao, J.; Guo, H.; Ha, S.; Joseph-McCarthy, D.; Kuchnir, L.; Kuczera, K.; Lau, F. T. K.; Mattos, C.; Michnick, S.; Ngo, T.; Nguyen, D. T.; Prodhom, B.; Reiher, W. E., III; Roux, B.; Schlenkrich, M.; Smith, J. C.; Stote, R.; Straub, J.; Watanabe, M.; Wiorkiewicz-Kuczera, J.; Yin, D.; Karplus, M. *J. Phys. Chem. B* **1998**, *102*, 3586–3616.

(23) Kucerka, N.; Tristram-Nagle, S.; Nagle, J. F. *J. Membr. Biol.* **2005**, *208*, 193–202.

(24) Woolf, T. B.; Roux, B. *Proc. Natl. Acad. Sci.* **1994**, *91*, 11631–11635.

(25) Woolf, T. B.; Roux, B. *Molecular dynamics of PfI coat protein in phospholipids bilayer in Biological Membranes: A Molecular Perspective from computation and experiment*; Merz, K. M., Roux, B., Eds.; Berkhauser: Boston, 1996.

(26) Heller, H.; Schaefer, M.; Schulten, K. *J. Phys. Chem. B* **1993**, *97*, 8343–8360.

(27) Pandit, S. A.; Scott, H. L. *J. Chem. Phys.* **2006**, *124*, 014708–7.

(28) Cournia, Z.; Vaiana, A. C.; Ullmann, G. M.; Smith, J. C. *Pure Appl. Chem.* **2004**, *76*, 189–196.

(29) Darden, T.; York, D.; Pedersen, L. *J. Chem. Phys.* **1993**, *98*, 10089–10092.

(30) Patra, M.; Karttunen, M.; Hyvonen, M. T.; Falck, E.; Vattulainen, I. *J. Phys. Chem.* **2004**, *108*, 4485–4494.

(31) de Almeida, R. F. M.; Fedorov, A.; Prieto, M. *Biophys. J.* **2003**, *85*, 2406–2416.

(32) Ivanov, I.; Vemparala, S.; PophristicKuroda, V. K.; DeGrado, W. F.; McCammon, J. A.; Klein, M. L. *J. Am. Chem. Soc.* **2006**, *128*, 1778–1779.

(33) Benz, R. W.; Castro-Roma, F.; Tobias, D. J.; White, S. H. *Biophys. J.* **2005**, *88*, 805–817.

(34) Hofsab, C.; Lindahl, E.; Edholm, O. *Biophys. J.* **2003**, *84*, 2192–2206.

(35) Zhu, Q.; Cheng, K. H.; Vaughn, M. W. *J. Phys. Chem. B* **2007**, *111*, 11021–11031.

(36) Róg, T.; Murzyn, K.; Garbiel, R.; Takaoka, Y.; Kusumi, A.; Pasenkiewicz-Gierula, M. *J. Lipid Res.* **2004**, *45*, 326–336.

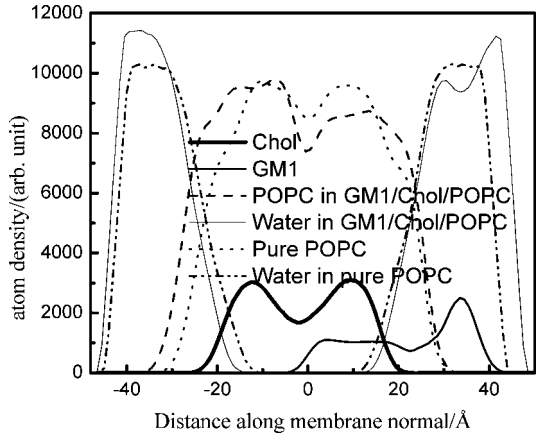

Figure 2. Atom density distribution of POPC, GM1, Chol, and water from ternary lipid bilayer. To compare the result the atom density of POPC and water from pure POPC bilayer is included.

bilayer along the membrane normal. It is clear from the figure that the influence of GM1 on the membrane asymmetry is restricted mostly at the water level. It is also observed that the distribution of Chol in the upper layer overlaps with the hydrophobic part of the GM1, indicating that the major interaction of GM1 with Chol is hydrophobic in nature.

Binary and ternary lipid mixtures have gel phase with liquid-ordered domains varying in size from nanometers to micrometers, surrounded by a fluid-disordered membrane. The coexistence of L_o and L_d phases are observed in a wide variety of three-component lipid membranes.[20,37−39] To look into the possibility of formation of "condensed complex" between GM1 and Chol we have taken snapshots of GM1 and Chol at regular time intervals, and the snapshots are shown in Figure 3A. For clarity we have kept only two GM1 molecules and the neighboring POPC and Chol molecules. The emergence of more ordered POPC molecules sequestered between two GM1 molecules as well as several Chol molecules stacking along the ceramide tails of GM1 are clearly visible. The analysis of the distribution and dynamics of these POPC and Chol molecules is given later. The sterol ring is seen to interact sideways with GM1 hydrophobic chain (Figure 3B). Though Chol has H-bond donor and acceptor groups, no direct H-bonding interaction of Chol with GM1 is observed. Only few water-mediated H-bonds between Chol and GM1 were observed (Figure 3C). Previous molecular dynamics simulation studies of SM/Chol/PC ternary lipid bilayer have reported formation of a H-bond between Chol and SM.[40] Holopainen et al.,[41] on the other hand, did not detect any specific interaction between SM and Chol using fluorescence spectroscopy. Formation of condensed complex as a result of nonpolar interactions has been supported from other evidence as well.[42−44] The origin of condensed complex is explained from the condensation of sphingomyeline monolayer in the presence of Chol where the interaction between Chol and SM is observed to be hydrophobic in nature. The snapshots of the trajectory indicate that the presence of GM1 may help the Chol moieties to get more ordered, and this might be a possible route through which GM1-Chol-lipid might form ordered domains. According to Hancock, the small L_o (which may be transient lateral assemblies of Chol and sphingolipids) domains might be expected to progressively coalesce into ever larger and eventually macroscopic domains once they are captured by the proteins,[7] i.e., these smaller subnanoclusters are the platform for formation of lipid rafts, which can facilitate protein−protein interaction by selectively including or excluding proteins. The snapshots of the trajectory clearly indicate the possibility of formation of Chol-rich regions near GM1 molecules.

To compare with the binary lipid system the snapshots of the lower layer containing only Chol are taken within the same time interval (Figure 3D). Figure 3D indicates that the tendency to form the Chol-rich domain is observed within 20 ns. However, the formed cluster breaks immediately after 30 ns simulation (Figure 3D). Comparison of Figure 3A and 3D can clearly indicate that the tendency to form stable Chol-rich domain is more in the GM1-containing upper layer. In binary POPC bilayer, Chol can form a Chol-rich domain at 33 mol % Chol concentration.[21]

The increased tendency to form Chol clustering can also be seen from the Chol-Chol radial distribution function [RDF] in both layers (Figure 4). The RDF is computed by calculating the average number of molecules available around a selected site.[45] Figure 4 indicates that the intensity is broader and higher for the upper layer compared to the lower layer. The height of the maxima increases approximately two times in the upper layer than the lower layer. This indicates that the local density of Chol increases in the upper layer. This suggests that the distribution of Chol is not uniform[40] in a ternary lipid system, which is in excellent agreement with a previous report where it was shown that Chol have preference for sphingolipid than phospholipids during domain formation.[46]

The orientations of the Chol and PN vectors with respect to the bilayer normal (Figure 5A and 5B) also shows that the distribution of the Chol vectors in the upper layer is narrower than that of the lower layer. We further separated the Chol molecules in the upper layer in two categories: those which are close to GM1 (within a radius of 6 Å) and the others outside the range. The distribution now indicates that the Chol moieties which are close to GM1 are oriented nearly parallel to the bilayer normal with an average tilt angle of 15° (Figure 5A). The Chol molecules that are not close to GM1 show an additional hump at 27°. The distribution of the PN vector shows (Figure 5B) that though in the pure bilayer the distribution is wide and symmetric around 90°, in the presence of GM1 the orientation of the PN vectors in both layers is affected. While in the upper layer it shows a broader distribution near 70°, in the lower layer a narrower distribution is seen round 80°. In the snapshots (Figure 3A) it is also seen that there are several POPC molecules placed in between two GM1 molecules. This makes some of the POPC molecules in the upper layer quite restricted, whereas the POPC molecules which are not in direct contact with GM1 are more disordered. This results in the observed broad distribution of the PN vectors in the upper layer, while in the lower layer POPC remains more ordered due to the presence of Chol molecules.

Formation of Chol-rich domain can be shown from calculation of the number of contacts between the lipid components with time.[35]

(37) Pandit, S. A.; Jakobsson, E.; Scott, H. L. *Biophys. J.* **2004**, *87*, 3312–3322.
(38) Yuan, C.; Furlong, J.; Burgos, P.; Johnson, L. J. *Biophys. J.* **2002**, *82*, 2526–2535.
(39) Kahya, N.; Scherfeld, D.; Bacia, K.; Poolman, B.; Schwille, P. *J. Biol. Chem.* **2003**, *278*, 28109–28115.
(40) Pandit, S. A.; Vasudevan, S.; Chiu, S. W.; Mashl, R. J.; Jakobsson, E.; Scott, H. L. *Biophys. J.* **2004**, *87*, 1092–1100.
(41) Holopainen, J. M.; Metso, A. J.; Mattila, J.; Jutila, A.; Kinnunen, P. K. J. *Biophys. J.* **2004**, *86*, 1510–1520.
(42) Radhakrishnan, A.; Anderson, R. G.; McConnell, H. M. *Proc. Natl. Acad. Sci.* **2000**, *97*, 12422–12427.
(43) Radhakrishnan, A.; Li, X.-M.; Brown, R. E.; McConnell, H. M. *Biochim. Biophys. Acta* **2001**, *1511*, 1–6.
(44) Li, X.-M.; Momsen, M. M.; Smaby, J. M.; Brockman, H. L.; Brown, R. E. *Biochemistry* **2001**, *40*, 5954–5963.
(45) Chiu, S. W.; Jakobsson, E.; Mashl, R. J.; Scott, H. L. *Biophys. J.* **2002**, *83*, 1842–1853.
(46) Hyvönen, M. T.; Kovanen, P. T. *J. Phys. Chem. B* **2003**, *107*, 9102–9108.

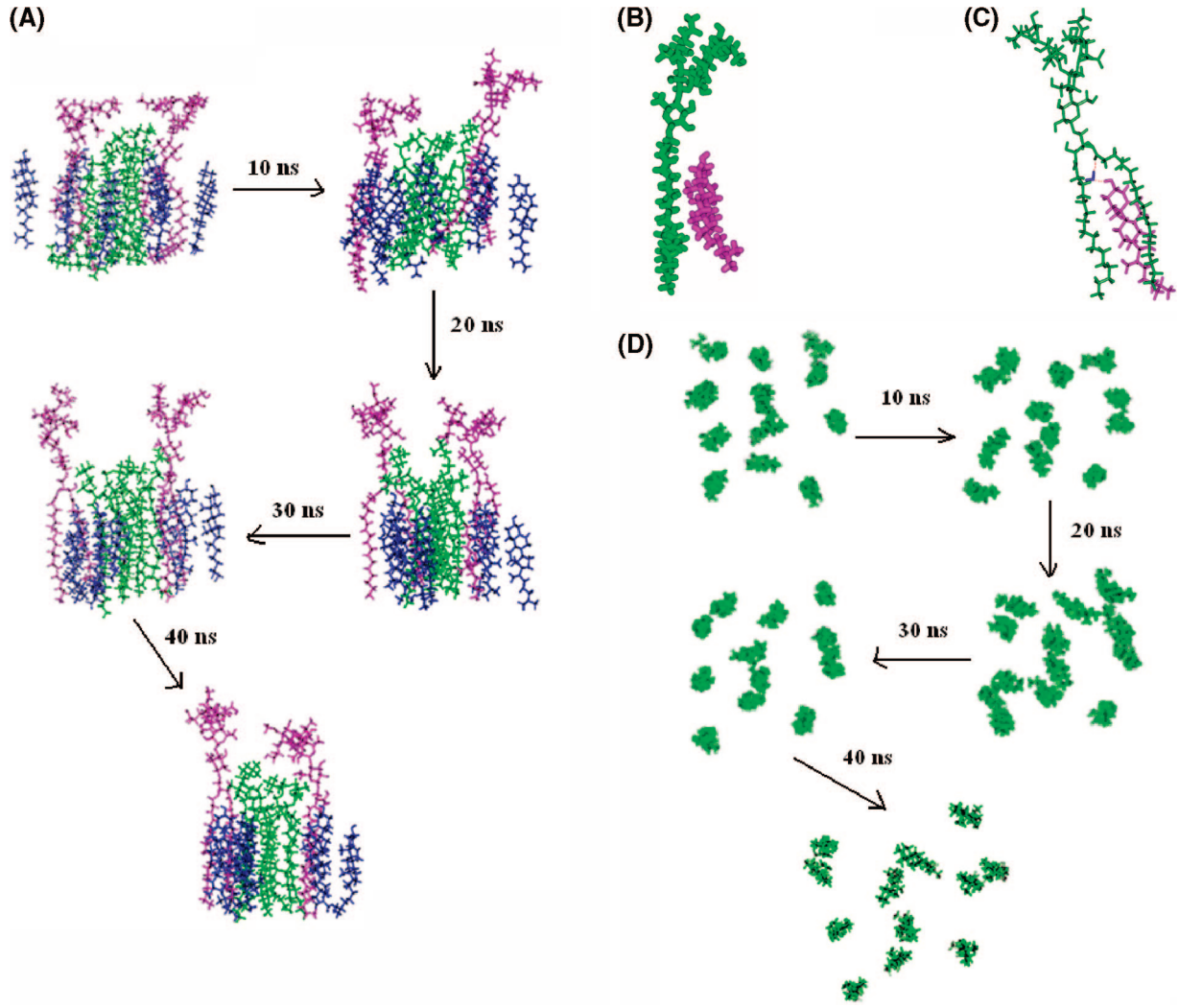

Figure 3. (A) Snapshots taken for POPC (green sticks), Chol (blue sticks), and GM1 (magenta sticks) from start to 40 at 10 ns time intervals representing stepwise organization of Chol around GM1 (upper layer) in ternary lipid bilayer. (B) van der Waals interaction and (C) water (blue) mediated H-bonding between GM1(green) and Chol (magenta) in ternary lipid bilayer. (D) To compare the data with Figure 3A, a snapshot of the lower layer containing only Chol (green sticks) at the same time interval is also given.

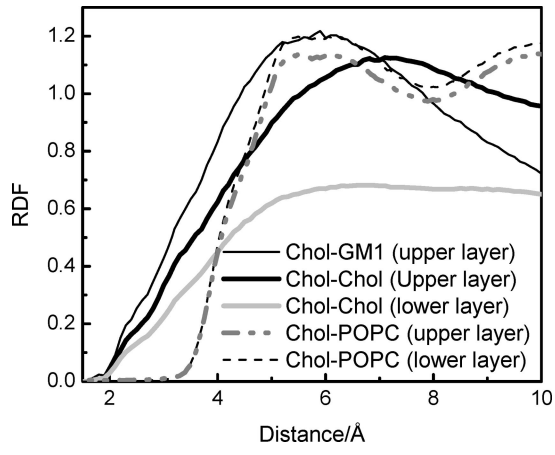

Figure 4. RDF plot for Chol-Chol and Chol-POPC in both the upper and lower layers from ternary lipid bilayer. The figure also includes Chol-GM1 RDF for the upper layer.

The number of contacts between the lipids is calculated by counting the number of lipid components present within a circle of 6 Å from the reference lipid molecule and averaged over all reference lipid molecules. We calculated the number of contacts between PC-Chol, PC-PC, and Chol-Chol in both the upper and lower layers separately (Figure 6A and 6B) for the last 20 ns simulation run. The number of contacts for PC-GM1 and Chol-GM1 are also included in Figure 6A. The number of PC-Chol contacts in upper layer (Figure 6A) is lower than that in the lower layer (Figure 6B), and the decrease is compensated by the increase in the number of Chol-Chol contacts in the upper layer. However, the PC-PC contacts in the upper and lower layers are almost the same. Again, the average number of GM1-Chol contacts is larger than the number of GM1-PC contacts though PC's are present in more numbers than Chol. Very recently Zhu et al. observed that the number of contacts between POPC-Chol at 40 mol % concentration increases with time and concluded that the Chol diffuses from Chol-rich domain to POPC-rich domain.[35] However, from our simulation (Figure 6A) we see that in the presence of GM1, Chol prefers to stay in the region rich in GM1, which is also predicted from the RDF of Chol around GM1, Chol, and POPC (Figure 4).

Calculation of the order parameter (S_{CD}) gives information about the extent of rigidity of the membrane interior.[47,48] The change of

(47) Moore, P. B.; Lopez, C. F.; Klain, M. L. *Biophys. J.* **2001**, *81*, 2484–2494.
(48) Róg, T.; Murzyn, K.; Garbiel, R.; Takaoka, Y.; Kusumi, A.; Pasenkiewicz-Gierula, M. *J. Lipid Res.* **2004**, *45*, 326–336.

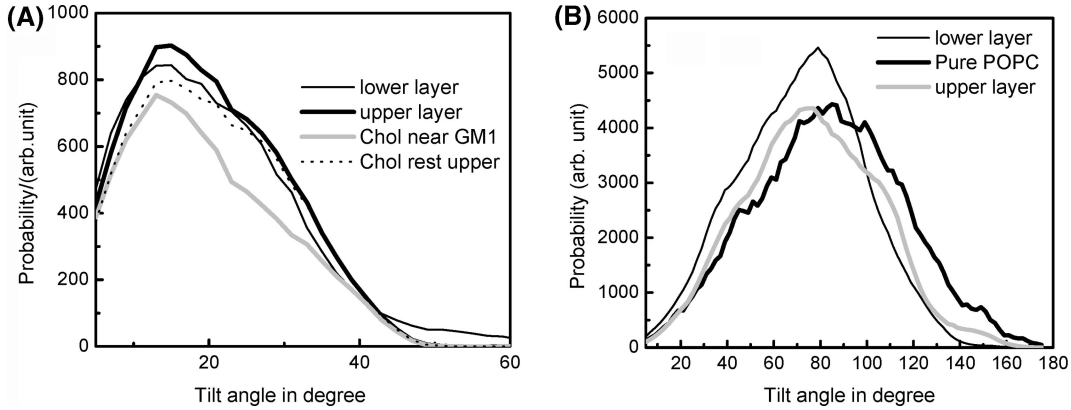

Figure 5. (A) Orientations with respect to the bilayer normal of the Chol ring vector for both the upper and lower layers of the ternary lipid bilayer. The distribution of the Chol ring vector around 6 Å from the GM1 is calculated as Chol near GM1 and outside that are included as rest Chol. (B) The distribution of PN vectors for both the upper and lower layers of the ternary lipid bilayer and pure POPC bilayer.

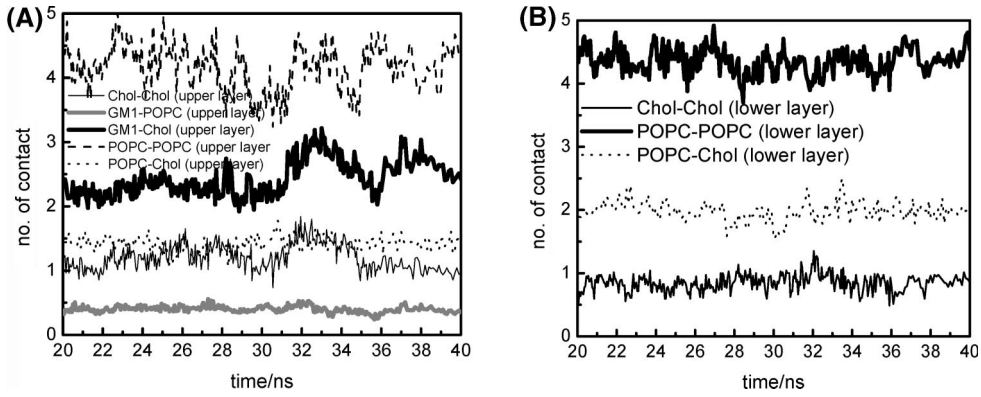

Figure 6. Average number of contacts between different lipid components calculated for the last 20 ns simulation time for different molecular pairs: (A) number of contacts between Chol-Chol, POPC-Chol, Chol-GM1, GM1-POPC, and POPC-POPC in the upper layer and (B) number of contacts between Chol-Chol, POPC-POPC, and POPC-Chol in the lower layer of the ternary lipid bilayer.

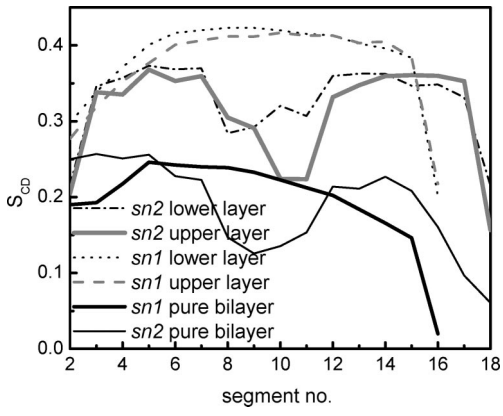

Figure 7. Order parameter (S_{CD}) for POPC of the upper and lower layers reported separately in the mixed bilayer along with the order parameter of pure POPC molecules. (To give the amount of ordering, the order parameter of a single POPC molecule near the cluster region in the upper layer is given).

S_{CD} indicates the extent of altered rigidity of membrane.[49] A value of 0.5 gives a totally ordered system, whereas the value is zero for a disordered system. Our previous data indicated that the presence of Chol increases S_{CD} for both chains of POPC.[21] From Figure 7 it is seen that the S_{CD} increases nearly two times the pure one, but the extent of ordering in the upper layer is less than the lower layer. In a three-component system containing PC/Chol and SM, the increase in S_{CD} has been reported.[37,50] The AFM experiment also reports increased ordering of the raft-like domains.[51] We calculated separately the value of S_{CD} for POPC near the GM1-Chol cluster (figure not shown) where the average value of S_{CD} for *sn1* chain ranges from 0.30 to 0.47 and for *sn2* chain from 0.20 to 0.45. The values are much larger than the average value observed for the POPC molecules in the upper layer. The increase in S_{CD} implies reduction of membrane fluidity, which is linked to the reduction of flexibility of acyl chains and formation of liquid-ordered domain. It is also observed from

Table 1. Diffusion Coefficient of Different Lipid Components

type of molecule	diffusion coefficients (D_t) in 10^{-8} cm^2/s
POPC in pure POPC bilayer[21]	11.93 ± 0.8
POPC in the upper layer of the ternary lipid bilayer	7.95 ± 0.10
POPC in the lower layer of ternary lipid bilayer	6.90 ± 0.06
POPC in ternary lipid bilayer	7.42 ± 0.2
POPC at 22 mol % Chol in binary mixture[21]	7.21 ± 0.01
POPC within the cluster in the upper layer of ternary lipid bilayer	4.8 ± 0.21
Chol in the upper layer of ternary lipid bilayer	4.53 ± 0.08
Chol in the lower layer of the ternary lipid bilayer	7.15 ± 0.06
Chol at 22 mol % Chol in binary mixture[21]	12.83 ± 0.1

(49) Seelig, A.; Seelig, J. *Biochemistry* **1974**, *13*, 4839–4845.
(50) Róg, T.; Pasenkiewicz-Gierula, M. *Biophys. J.* **2006**, *91*, 3756–3767.
(51) Rinia, H. A.; Snel, M. M. E.; van der Eerden, J. P. J. M.; de Kruijff, B. *FEBS Lett.* **2001**, *501*, 92–96.

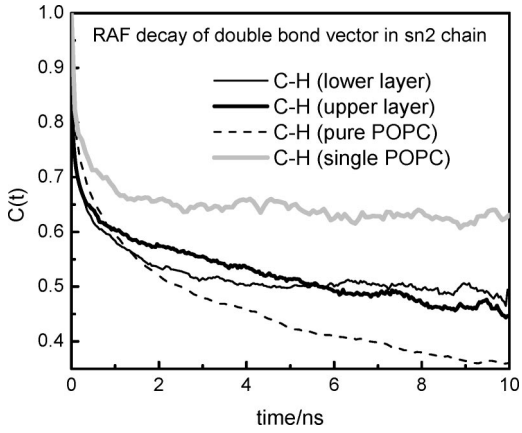

Figure 8. Decay of rotational relaxation of a selected POPC C−H vector (C−H) in both the upper and lower layers of mixed bilayer along with the C−H vector of pure POPC bilayer. To account the organization of Chol near GM1, the RAF of the C−H vector of a single POPC near the cluster region in the upper layer is also included.

Figure 7 that the value of S_{CD} for POPC molecules in the upper layer is slightly lower than those in the lower layer, which is in accordance with the previous observation of PN vector distribution (Figure 5B). In the upper layer formation of a small cluster containing GM1-Chol and POPC leaves some of the POPC molecules less ordered.

The lateral mobility of POPC and Chol molecules can be estimated from their translational diffusion coefficients (D_t).[52] The diffusion coefficients, obtained from the slope of the time series of the mean square displacement of the center of mass in the membrane plane for POPC and Chol, are indicated in Table 1. The lateral diffusion constant of POPC, measured in multilamellar liposome's using pulsed field gradient magic-angle spinning (PFG-MAS) ^{1}H NMR at 322 K, has a value of $(8.6 \pm 0.2) \times 10^{-8}$ cm^2/s when dehydrated (8.2 waters/lipid) and $(19.0 \pm 0.1) \times 10^{-8}$ cm^2/s in excess water.[53] The D_t for POPC in pure bilayer is $(11.93 \pm 0.8) \times 10^{-8}$ cm^2/s,[21] which agrees fairly well with the experimental data. For the present system the diffusion coefficients calculated for POPC in the upper and lower layers separately are $(7.95 \pm 0.10) \times 10^{-8}$ and $(6.90 \pm 0.10) \times 10^{-8}$ cm^2/s, respectively. We previously reported D_t of POPC and Chol from the binary bilayer simulation with 22 mol % Chol concentration,[21] which is similar to the present study (~25 mol %). From Table 1 it is clear that the D_t of POPC in the binary system (i.e., in the Chol-POPC system as well as in the lower layer of the present study) is similar. However, in the ternary system, i.e., the upper layer of the GM1/Chol/POPC system, the value increases slightly to 7.95×10^{-8} cm^2/s. The increase in D_t for PC in the upper layer is again indicative of a relatively more disordered arrangement of POPC in the upper layer as suggested earlier. The average D_t of the POPC molecule within the GM1-Chol cluster represented in Figure 3A is $(4.8 \pm 0.21) \times 10^{-8}$ cm^2/s, which is significantly smaller than the average value of the diffusion coefficient in the upper layer [$(7.95 \pm 0.1) \times 10^{-8}$ cm^2/s]. The simultaneous presence of ordered and disordered domains are thus shown. Table 1 also shows that D_t of Chol is significantly reduced in the ternary layer as compared to that in the binary bilayer having a comparable Chol concentration (22 mol %).[21] Comparison of D_t of Chol between the upper and lower layers indicates that the value of the diffusion coefficient is larger in the lower layer for Chol, i.e., Chol has higher mobility in the layer without GM1.

(52) Czub, J.; Baginski, M. *Biophys. J.* **2006**, *90*, 2368–2382.

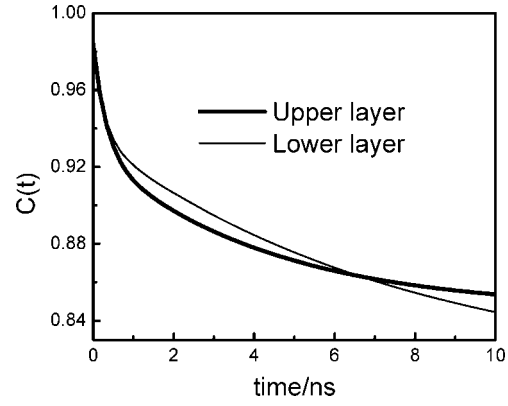

Figure 9. Decay of the RAF of the sterol ring vector for the Chol molecules present in the upper (thick line) and lower layers (thin line) separately.

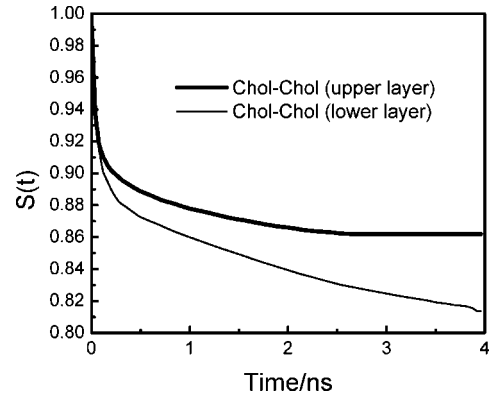

Figure 10. Decay of the survival time correlation function [$S(t)$] for Chol molecules with respect to Chol for the upper (thick line) and lower layers (thin line).

The amount of rigidity within the membrane bilayer can be traced from calculation of the rotational autocorrelation function (RAF) of selected CH vectors of acyl chains. The extent of decay of RAF depicts the restriction of rotation of the respective vector. The RAF is calculated from the equation[54]

$$C(t) = \langle P_2[\mu(0)\mu(t)] \rangle \quad (1)$$

where $\mu(t)$ and $\mu(0)$ are the vectors joining the pairs C_j-C_{j-1} and C_j-C_{j+1} at time t and beginning and P_2 is the second-order Legendre polynomial. The calculation is averaged over different time origins and over all the molecules. The data of RAF for the CH vector of *sn2* chain double bond is plotted in Figure 8. As the decay after 1 ns becomes parallel with time axis, the 1 ns time scale is sufficient for calculation of the RAF decay for POPC. The figure shows that the decay becomes slower in GM1-containing system. To quantize the restriction in rotation we calculated the time of decay by fitting a biexponential decay with a fixed part as follows

$$C(t) = A_0 + A_1 e^{-(t/\tau_1)} + A_2 e^{-(t/\tau_2)} \quad (2)$$

where A_1 and A_2 are fractions of the fast and slow components of motions to the decay and A_0 is a constant indicating the stable component of decay and indicative of restriction of rotation in membrane environment. The reorientational correlation time τ_1 and τ_2 along with their relative contributions A_1, A_2, and a constant component A_0 have been shown (Table 2). The data indicates that the presence of GM1 influences both the shorter and longer components of decay time. The constant part of the fitting parameter is also larger for GM1-containing bilayer. This clearly

Table 2. Fitting Parameters for the Rotational Autocorrelation Function

system	A_0	A_1	τ_1 (ns)	A_2	τ_2 (ns)
sn2 chain vector (upper layer)	0.43	0.33	0.06	0.22	5.12
sn2 chain vector (lower layer)	0.50	0.30	0.05	0.20	1.24
sn2 chain vector (selected POPC in the upper layer)	0.52	0.28	0.07	0.20	6.78
sn2 chain vector (pure POPC bilayer)	0.32	0.35	0.16	0.33	4.51
sterol ring (lower layer)	0.81	0.05	0.26	0.12	7.76
sterol ring (upper layer)	0.85	0.07	0.31	0.08	3.95

shows the restriction of rotation in the presence of GM1. The rotational restriction of lipid molecules increases more in mixed bilayer ($A_0 = 0.43$ and 0.50) than pure POPC molecules ($A_0 = 0.32$), whereas shorter components are much faster ($\tau_1 = 0.06$ and 0.05 ns with $A_1 = 0.33$ and 0.30) than pure POPC molecules ($\tau_1 = 0.16$ ns with $A_1 = 0.35$). The longer component of decay is slower for the upper layer ($\tau_2 = 5.12$ ns with $A_2 = 0.22$) than the lower layer ($\tau_2 = 1.24$ ns with $A_2 = 0.20$). This result indicates a complex dynamics of the RAF in the presence of GM1. The dynamics of POPC molecules in the region of cluster is more restricted as compared to the average value (Table 2). The constant component ($A_2 = 0.52$) and longer decay time ($\tau_2 = 6.78$ ns) indicates more restriction of the cluster region than the upper layer.

Due to formation of Chol-GM1 assembly the rotational restriction of the Chol ring increases. This increase in rotational restriction can be shown from calculation of decay of the rotational autocorrelation function of the sterol ring plane vector with time (Figure 9). The fitting parameter for the decay is given in Table 2, and data indicate a complex rotational dynamics of the sterol ring in the presence and absence of GM1. The constant component of the decay indicates that the rotational restriction of Chol is more for the upper layer ($A_0 = 0.85$) as compared to the lower layer ($A_0 = 0.81$). The short component of the decay time is also greater for the upper layer ($\tau_1 = 0.31$ ns as compared to 0.26 ns for lower layer) with almost equal fractional contribution ($A_1 = 0.07$ and 0.05), whereas a slower decay time is larger for the lower layer ($\tau_2 = 7.76$ ns) than the upper layer ($\tau_2 = 3.95$ ns). This imposes a minimum effect as the fractional contribution for the upper layer ($A_2 = 0.08$) is lower than the lower layer ($A_2 = 0.12$).

The probability of the existence of Chol-Chol clustering can be visualized from the survival time correlation function of Chol within a sphere of radius of 5 Å around a Chol molecule by the equation[54]

$$S_R(t) = \frac{1}{N_w}\sum_{j=1}^{N_W}\frac{\langle P_{Rj}(0)P_{Rj}(t)\rangle}{\langle P_{Rj}(0)^2\rangle} \quad (3)$$

where P_{Rj} is a binary function that takes the value of 1 if the *j*th Chol molecule stays in the layer of thickness *R* for a time *t* without getting out during this interval and of zero otherwise. Figure 10 shows the nature of the survival time, and we can see that the decay is slower in the upper layer, which indicates that the tendency of Chol-Chol cluster formation, lifetime of cluster, is more in the presence of GM1. The correlation times (Table 3) are obtained by fitting a biexponential curve along with a fixed component, given by eq 2. Table 3 indicates that the constant part for the Chol-Chol survival time correlation function for the upper layer is more than the lower layer [$A_0 = 0.86$ and 0.79, respectively], indicating more restriction for the residence time decay in the presence of GM1. The short decay times are more or less equal [$\tau_1 = 0.04$ and 0.06 ns] with an equal fractional contribution [$A_1 = 0.09$ and 0.10], but the longer component differs significantly [$\tau_2 = 0.92$ and 2.69 ns, respectively, for the upper and lower layers].

Table 3. Fitting Parameter for Survival Time Decay

system	A_0	A_1	τ_1(ns)	A_2	τ_2 (ns)
Chol-Chol (lower layer)	0.79	0.11	0.06	0.1	2.69
Chol-Chol (upper layer)	0.86	0.09	0.04	0.05	0.92

The entire analysis indicates formation of Chol-rich domain in the presence of GM1. The organization of Chols in the presence of sphingolipids into ordered lipid domains is promoted due to the interaction between Chol and the long ceramide moieties of the sphingolipids. An earlier report indicates that within sphingolipids ceramide shows strikingly higher affinity for ordered phases.[55] Though a different headgroup of sphingolipids gives a different extent of ordering, the net domain formation is not directly dependent on the headgroup composition.[55] Calculation of the diffusion coefficient and RAF indicates the reduced mobility of Chol in the upper layer as compared to the lower layer. It is also noted that a few POPC molecules which become part of the Chol-GM1 assembly have reduced translational and rotational mobility. Our simulation supports the idea that phase separation is facilitated due to the presence of GM1. The molecular dynamics simulation gives that in ternary phase system, the main component responsible for phase separation is Chol. Thus, detailed understanding of the simulation result gives us a clear picture about how Chol participates in phase separation.

Conclusion

Molecular dynamics simulation is a powerful tool to probe the structural and dynamical properties of membranes at the atomic level. The system size and simulation time are two important factors for such simulations. Application of periodic boundary condition reduces the size effect. Formation of stable lipid raft is a long time-scale process and not accessible to nanosecond all-atom simulations. We report here the initial events of membrane organization in the ternary lipid bilayer focusing only on the membrane properties which are relatively localized and fast. Rotational relaxation, survival time, and lateral diffusion fall within the current limit. The present study is an attempt to elucidate some of the structural and dynamical fluctuations of lipid bilayers in the ternary phase and compares with binary and pure lipid bilayer on the order of several nanoseconds simulation times.

On formation of lipid cluster accompany several structural and dynamical changes which directly affects the flexibility of the surrounding PCs and with increasing complexity of the lipid bilayer, the correlation between membrane structure/dynamics with membrane composition becomes complicated. We have shown here the organization of 6 Chol moieties around 2 GM1 molecules sequestering in between 4 POPC's, leading to formation of a lateral assembly. The dynamic nature of the constituent POPC and Chol's is quite different from that of the counterparts which are not part of the assemblies. The major interaction between GM1 and Chol is observed to be hydrophobic in nature. We report that formation of subnanocluster in ternary lipid mixture is more favorable than in binary lipid mixture. From our simulation in nanosecond order and ternary lipid bilayer we are able to give an idea about the initial stages of domain formation which can help to understand the initial events that occur during lipid raft formation.

Acknowledgment. This work was partially supported by the Council for Scientific and Industrial Research (No. 01(2035)/06/EMR-II) Government of India.

LA8015589

(53) Gaede, H. C.; Gawrisch, K. *Biophys. J.* **2003**, *85*, 1734–1740.
(54) Rocchi, C.; Bizzarri, R A.; Cannistraro, S. *Phys. Rev. E* **1998**, *57*, 3315–3325.
(55) Wang, T.-Y.; Silvius, J. R. *Biophys. J.* **2003**, *84*, 367–378.